

Ground-penetrating radar and electrical resistivity tomography for mapping bedrock topography and fracture zones: a case study in Viru-Nigula, NE Estonia

Ivo Sibul^{a,b}, Jüri Plado^a and Argo Jõelet^a

^a Institute of Ecology and Earth Sciences, University of Tartu, Ravila 14A, 50411 Tartu, Estonia; ivo.sibul@ut.ee

^b Estonian Land Board, Mustamäe tee 51, 10621 Tallinn, Estonia

Received 30 December 2016, accepted 7 April 2017, available online 26 June 2017

Abstract. The Geological Base Map (GBM), presenting an elongated buried valley running beneath the Varudi bog, triggered the geophysical studies near Viru-Nigula borough in northeastern Estonia. After the Geological Survey of Estonia had compiled the GBM map set, the course and extent of the valley still remained indistinct. Principally the morphology of the Varudi valley had been determined just by one borehole characterizing the 30 m thick Quaternary succession within the valley. The thickness of Quaternary sediments is, however, just a few metres in adjacent boreholes. We used ground-penetrating radar and electrical resistivity tomography (ERT) for acquiring extra knowledge about the extent and morphology of the Varudi structure. Ground-penetrating radar enabled us to specify the thickness and composition of Quaternary deposits, and to recognize dislocations of the bedrock blocks. As the radar images provided information on the topmost ~4 m only, ERT (Wenner and Wenner–Schlumberger arrays) was applied to define deeper, down to 40 m, electrical resistivity anomalies. The ERT studies revealed two fracture zones where regular Ordovician carbonate beds have been crushed and replaced by Quaternary sediments. The Varudi valley coincides with the southern zone. Both fracture zones probably acted as groundwater flow channels and sediment pathways in the Late Pleistocene, and hence supported the creation of the Varudi bog.

Key words: geological mapping, buried valley, fault, ground-penetrating radar, electrical resistivity tomography.

INTRODUCTION

Estonia is located on the southern slope of the Fennoscandian Shield. The geological layout of the country is generally divided into three structural stages: (i) Palaeo- and Mesoproterozoic crystalline basement (from the Orosirian to the Calymmian periods), (ii) Neoproterozoic and Palaeozoic sedimentary succession (from the Ediacaran to the Devonian period) preceded by a 0.8 Ga sedimentary hiatus and (iii) unconsolidated Quaternary sediments (Raukas 1997; Suuroja et al. 2006; Kirs et al. 2009). According to the national borehole database, managed by the Estonian Land Board, thousands of boreholes have been drilled into the Estonian bedrock, yet only about 500 of them reach the crystalline basement. Most of the boreholes are located in northern and northeastern Estonia due to the previous exploration of mineral resources (mainly oil shale and phosphorite).

Both the crystalline basement and the covering sedimentary bedrock are articulated by numerous faults, commonly related to the Caledonian orogeny. The faults occasionally intersect each other and form up to 4 km

wide systems while their vertical amplitude does not exceed 50 m (Puura & Vaher 1997). Because of the intensive exploration, most of the fault systems, oriented generally from NE to SW, are located in northern and northeastern Estonia (Fig. 1A). Glaciotectonics is another typical cause of faulting: remarkable dislocations within carbonate rocks have assembled to the south of the Baltic Klint (an outstanding erosional limestone escarpment along the northern coast of Estonia) where the fractured limestone was efficiently displaced by glaciers (Rattas & Kalm 2004; Plado et al. 2016).

The total thickness of the Estonian sedimentary bedrock complex increases southwards with an average dipping of 2–4.5 m per kilometre (Sildvee & Vaher 1995). The thickness of the Quaternary overburden is rather irregular: while totally missing on alvars, it may exceed 200 m in buried valleys (Raukas & Kajak 1995). Those valleys, eroded into the bedrock by glaciers and their meltwaters, are usually filled with glaciofluvial or glaciolacustrine deposits or tills in combination with glacio-aquatic deposits (Raukas & Kajak 1997). Before the Quaternary period the formation of the bedrock

© 2017 Authors. This is an Open Access article distributed under the terms and conditions of the Creative Commons Attribution 4.0 International Licence (<http://creativecommons.org/licenses/by/4.0>).

topography was controlled by tectonic processes and denudation. The course of the river valleys is often associated with tectonic structures – fracture zones were more easily affected by erosion and karst processes than continuous strata (Tavast 1997). The present relief usually follows the morphology of the bedrock relief (Kalm & Gorlach 2014), yet the tectonic structures

articulating the bedrock topography are rarely visible on the ground (Tavast 1997). Geophysical data, e.g. gravity, electric resistivity anomalies, enable the identification of the valleys eroded into relatively dense carbonate rocks filled with less dense glacial deposits (Tavast 1995) and specification of the origin of the landforms and structural elements (Vaher et al. 2013).

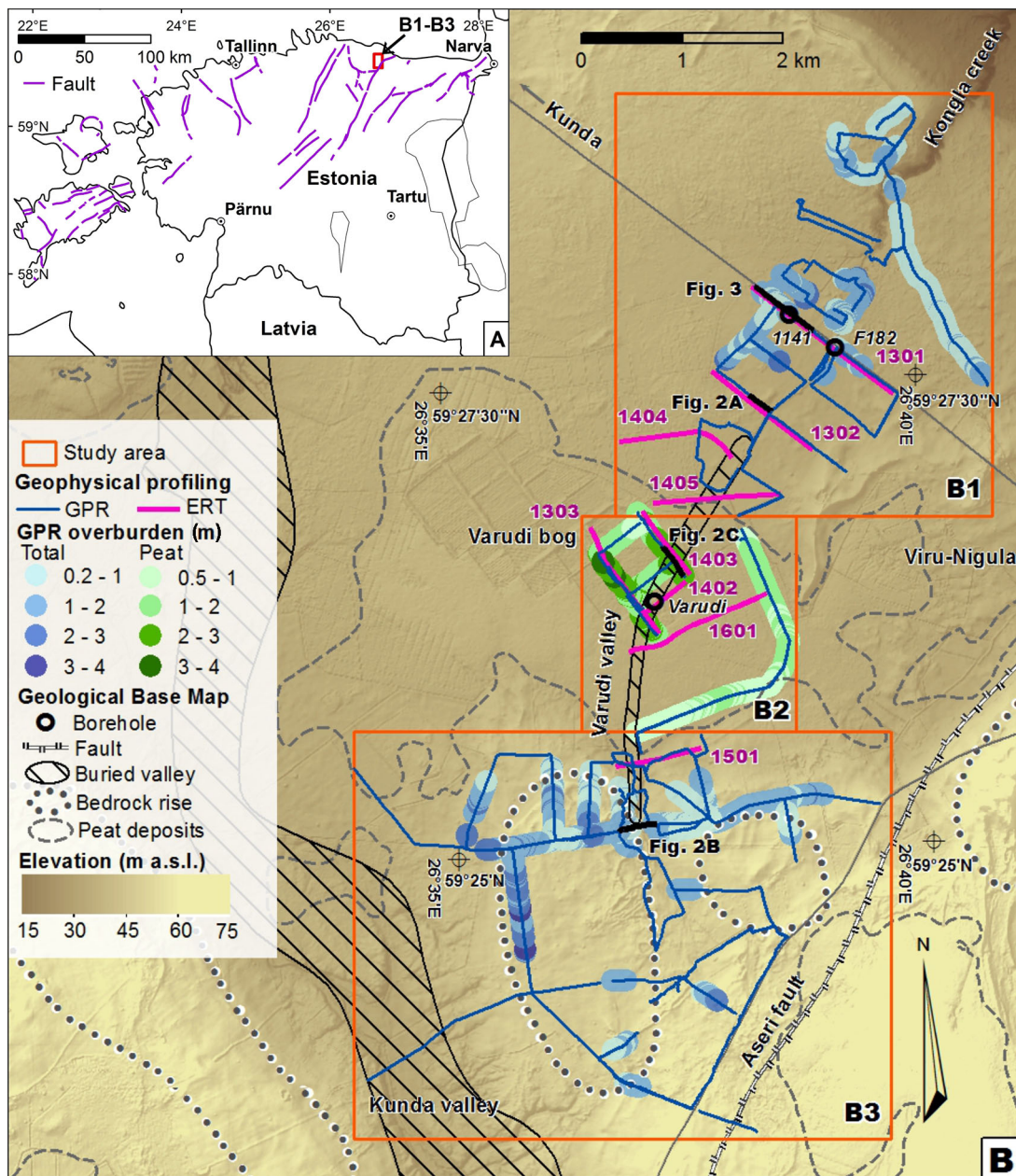


Fig. 1. A, geographical location map showing the main fault systems. B, geophysically profiled locations in the study area. For the areas B1 & B3 and B2 the total thickness of the Quaternary overburden and peat thickness interpretations are given, respectively. Thick black lines show the GPR profiles described in Figs 2 and 3. Boreholes and other objects from the Geological Base Map (GBM) are displayed on top of the digital elevation model (GBM and Lidar elevation data from the Estonian Land Board).

Current studies were induced by the results of the large-scale (1 : 50 000) geological base mapping (GBM) nearby the Viru-Nigula borough. The core of the Varudi borehole, where the Ordovician bedrock is covered with an unusually thick Quaternary succession, led the mappers to the assumption of a buried valley beneath the Varudi bog (Suuroja et al. 2006). Our aim was to clarify the extent of the assumed valley and the geological framework in the surroundings by geophysical (ground-penetrating radar [GPR] and electrical resistivity tomography [ERT]) approaches.

STUDY AREA

The study area is located in northeastern Estonia about 10 km south of the coast of the Gulf of Finland and the Baltic Klint (Fig. 1A). In the Kongla creek valley, north of the Varudi bog, the present relief is about 20 m a.s.l. Generally, the terrain ascends southwards, reaching 70 m at the bedrock rises (Fig. 1B). The crystalline basement (~170 m b.s.l.; Suuroja et al. 2006) is mainly composed of Palaeoproterozoic gneisses covered by Ediacaran sandstones, siltstones and clays. The subsequent Palaeozoic sequence embodies Cambrian and Ordovician strata, including limestones of the Middle Ordovician Vão and Kõrgekallas formations lying beneath the Quaternary overburden. The Quaternary succession, primarily shaped by the Late Weichselian glaciations, is diversified: till, glaciolacustrine clay, sand of different grain size, gravel, lacustrine lime, bog and fen peat have been mapped in the region (Suuroja et al. 2006). Sand and gravel, mostly of glaciofluvial origin, were deposited on top of till or carbonate bedrock. After the decline of the Baltic Ice Lake lacustrine sediments (lime and gyttja up to 1 m in thickness) were deposited into the Varudi depression, followed by peat accumulation in the Holocene (Suuroja et al. 2006). Nowadays the Varudi bog is partly an actively harvested field with a few metres of peat.

The study area (Fig. 1) was divided into three parts: (B1) an area with a thin Quaternary overburden around the Viru-Nigula–Kunda road, (B2) the Varudi bog, (B3) an area with a thin overburden at the bedrock rises south of the Varudi bog. According to GBM, the average thicknesses of the overburden in B1, B2 and B3 are 0–2, ~5 and 1–2 m, respectively.

A total of 114 data points (boreholes, pits and outcrops) have been described on the GBM in the areas B1–B3, about half of them entering the bedrock. The description of the 33 m deep Varudi borehole in the sector B2 is unique: Lower Ordovician sandstones, shales and clays are covered by Late Pleistocene till (27 m

and Holocene peat (3 m), whereas the typical Middle Ordovician limestones found in the neighbouring boreholes are missing (Suuroja et al. 2006).

DATA ACQUISITION AND PROCESSING

The GPR surveys (total length 66 km, Fig. 1) were carried out in 2012–2014 using a common offset co-polarized 300 MHz sled-mounted shielded antenna (Zond 12e; Radar Systems Inc.). Distances were measured using an odometer wheel attached to the rear of the sled. The profiles were positioned with a portable GPS unit (Altina GGM309; position accuracy 5–25 m) connected to the GPR system. The data were recorded using 200–300 ns time windows and post-processed with the Prism2 software including: (i) time-zero adjustments, (ii) signal saturation corrections (band-pass filter) for removing low-frequency (<100 MHz) induction effects and (iii) fitting hyperbolas to the point source reflections and diffractions for determining the electromagnetic wave velocities. Based on the velocity data, time was converted into the depth scale using a relative permittivity value 9 for limestone, 16 for sand and gravel, 32 for glacial till and 70 for peat deposits. Topography was corrected according to the airborne Lidar data provided by the Estonian Land Board.

The interpretation of the GPR images consisted of determining the Quaternary sediment types and searching the contact between the Ordovician carbonate bedrock and overburden. If identifiable, the bedrock top coordinates and depth were recorded with an average interval of 5 m along the profiles. The point data were then imported into the ArcGIS environment where the thickness values of the overburden were organized into symbol classes with an interval of 1 m.

The geoelectrical data of nine ERT profiles (Fig. 1) were collected between the years of 2013 and 2016 using a POLARES resistivity meter (P.A.S.I. srl). The 2D surveying method was considered suitable for the studies as the anticipated geological structures are elongated. The results of our earlier ERT and GPR campaigns were used to guide the location of the later lines. The individual lengths of the ERT profiles were 555–1755 m. Surveys were conducted mostly with a Wenner array, except for ERT_1303 (Fig. 1) which was performed with a Wenner-Schlumberger array, at a frequency of 7.2 Hz. Forty-eight steel electrodes with a constant spacing of 5 m were used simultaneously, with the alternation of two current and two potential electrodes and a roll-along survey by 32-electrode overlap. Such a technique provided a maximum exploration depth close to 40 m. Every 16th electrode was located by a hand-

held GPS device. Although the relief was rather flat along the profiles, Lidar-derived topography (from the Estonian Land Board) was applied in the processing.

After removing the erroneous data points and averaging repeated measurements, the apparent electrical resistivity data were tomographically inverted into the ‘true’ electrical resistivity distributions using the RES2DINV software package (Loke & Barker 1996). The software ran the optimization that adjusted the 2D electrical resistivity model by trying to reduce iteratively the difference between the calculated and measured apparent electrical resistivity values. Least-squares inversion (L1 norm) was applied identically to all the data for five iterations. The absolute root-mean-square error, providing a measure of convergence between measured and calculated data and, thus, indicating the reliability of the final result, ranged from 2.1% to 4.6%.

RESULTS

The GPR images revealed three major radar facies (RF1–RF3) in the Quaternary overburden and one (RF4) corresponding to the layered Ordovician carbonate rocks.

Within **RF1** the electromagnetic (EM) signals are attenuated in the topmost 2 m. Such a reflection pattern with no distinctive layering is typical for glacial till (Doolittle & Butnor 2009). The shallow signal penetration is related to the high electric conductivity of till that blocks the EM signal efficiently. The till beds lying directly on top of the carbonate bedrock often contain boulders, which are represented in radar images as hyperbolic features in the more homogeneous matrix.

The facies **RF2** is generally characterized by differently inclined and elongated occasional hyperbolic point reflections (Fig. 2A, B), and in some cases by the sub-parallel consistent layering (Fig. 2C). The facies RF2 was interpreted as an interstratified sand and gravel complex, which is generally laid on top of RF1. The fragmentary nature of RF2 reflections may associate with the alternating (glaciofluvial) deposition, whereas the continuous beds probably refer to a more stable (glaciolacustrine) environment (Fig. 2B). In the area B1, RF2 is traceable to the depths of 3–3.5 m (at relative permittivities of 14–18; Fig. 2A).

The facies **RF3**, registered in the area B2 to a depth of 2.5 m (at the average relative permittivity of 70), was interpreted as a peat complex without significant

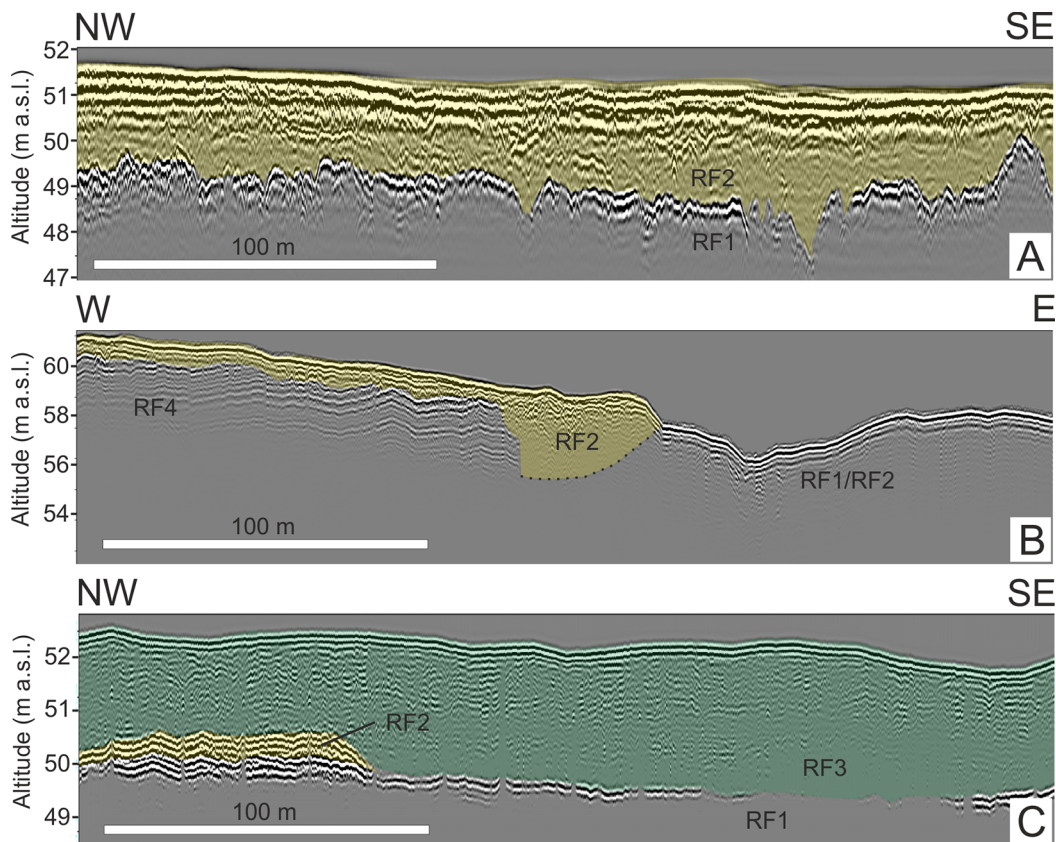


Fig. 2. A–C, radar images and interpretations of the GPR profiles; for locations see Fig. 1. In A, RF1 (till) is covered by RF2 (sand); in B, RF1/RF2 is underlain by RF4 (Ordovician carbonate bedrock); in C, RF1 is overlain by RF2 and RF3 (peat).

interbeddings (Fig. 2C). Peat is usually underlain by the sediments of much lower permittivity (e.g., RF2). Its bottom surface is therefore sharply displayed in radar images.

Another remarkable change in the physical properties of the subsurface occurs below the units RF1 and RF2. In about 40% of the images **RF4** was identified as the Ordovician carbonate bedrock complex (with the average relative permittivity of 9). The facies RF4 is typically represented by parallel subhorizontal reflections which are hundreds of metres long (Fig. 2B). The parallel reflections are caused by a variable clay content within the individual layers and layer surfaces (Mustasaar et al. 2012). In the rest of the images (i) the bedrock top remains too deep for recognizing (e.g. in the area B2), (ii) the EM signals are depleted by well-conductive sediments like RF1, or (iii) RF4 cannot be unequivocally distinguished from RF1.

The thickness of the Quaternary overburden in the northern part of the sector B1 does not exceed 2 m with one exception: in the Kongla creek valley the bedrock top is not detectable due to intensive alluvial deposition. Between boreholes 1141 and F182 (Figs 1, 3), the gap in the GPR-derived Quaternary thicknesses reaches ~500 m. In the southern part of the sector B1 as well as in the whole B2 (i.e. the eastern part of the Varudi bog), the bedrock top is untraceable due to (i) the EM signal depletion within RF1 or (ii) a relatively thick Quaternary succession (Fig. 1). In the bog and adjacent areas, the bottom surface of RF3 is clearly recognizable, usually underlain by RF1 or RF2 (Fig. 2C).

Within the area B3, the Quaternary thicknesses range from 0 to 4 m at relatively short (less than 30 m) distances. The northern slopes of the bedrock rises have

a thin (<2 m) Quaternary overburden while in general the thickness values increase southwards. In some radar images bedrock dislocations, probably caused by glaciotectonic processes, were registered. Similarly to the area B1, the bedrock top surface is unidentifiable in case the Quaternary sequence thickens over 4 m (Fig. 1).

The inversion of the ERT data resulted in nine sections (Figs 3, 4) with resistivity values mainly between 40 and 1400 Ωm. The resistivity distribution includes four resistivity units (RU1–RU4).

The thin (2–12 m) topmost unit **RU1** corresponds to Quaternary sediments and has resistivity mostly <250 Ωm. Occasionally, e.g. the line ERT_1404 at the distances between 300 and 900 m, the unit is divided into two parts, upper and lower (Fig. 4). The upper part has usually higher resistivity corresponding to variations in sedimentary compositions and/or electrical resistances.

Considering the local geological section, results of the earlier drillings (Fig. 1) and electrical resistivity of the Estonian sedimentary rocks (Jõelet & Kukkonen 2002), **RU2**, a 15–20 m thick unit with relatively high (>350 Ωm) resistivity corresponds to Middle Ordovician carbonate rocks.

The lowermost unit **RU3** (15 m thick), with resistivity generally between 100 and 400 Ωm, matches with Lower Ordovician and Cambrian sandstones, shales and clay described by Suuroja et al. (2006).

The above-described electrical sections (RU1–RU3) are broken by vertical zones having low resistivity (generally <100 Ωm), denoted as **RU4**. We suggest that these 70–450 m wide zones (Figs 3, 4) correspond to fractured Ordovician bedrock with a high fluid content responsible for good electrical conductivity, but

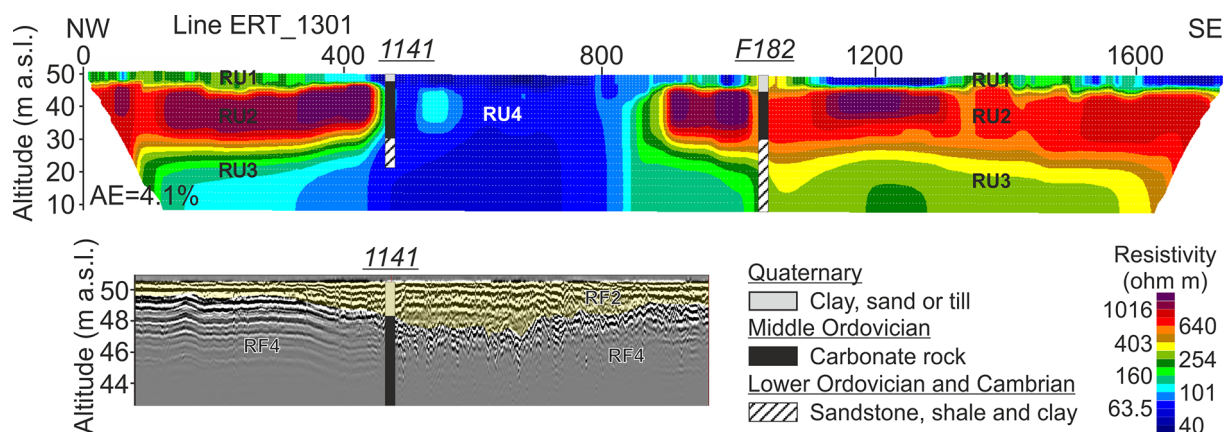


Fig. 3. Electrical resistivity image along the line ERT_1301 (above) juxtaposed with the coinciding GPR image (below; for locations see Fig. 1). In the ERT image the intervals 0–450 and 900–1755 m correspond to the Quaternary cover and homogeneous bedrock, at the distance of 450–900 m the resistivity values drop abruptly. Simplified lithological columns are given for boreholes 1141 and F182 (for locations see Fig. 1).

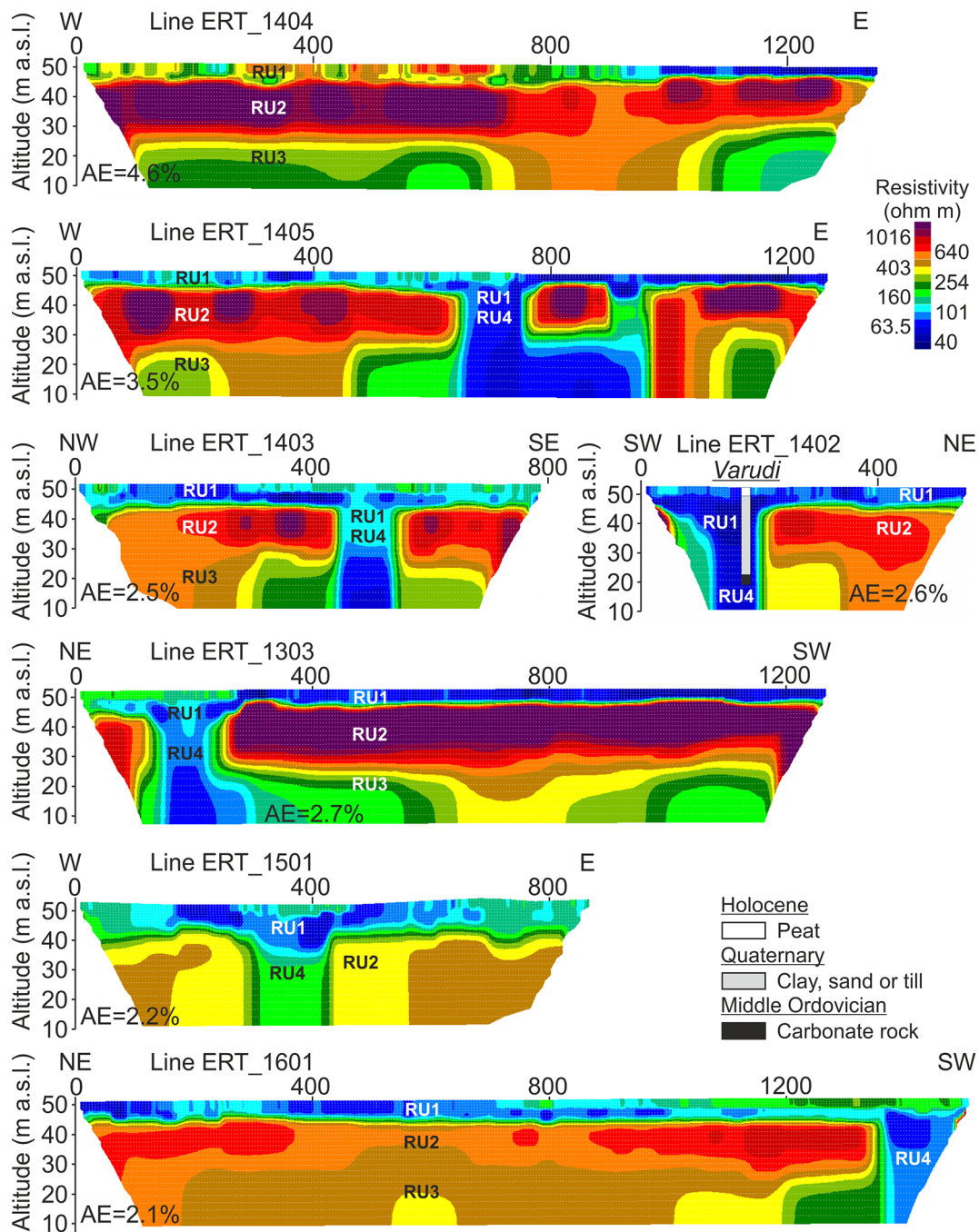


Fig. 4. Electrical resistivity images along the seven ERT lines (for locations see Fig. 1). A simplified lithological column is given for the Varudi borehole on the line ERT_1402. Resistivity values show strong contrast between the various lithologies (see text) and reveal fracture zones as vertical anomalously low-resistivity areas.

the Quaternary sediments may also have contributed (see, e.g., the line ERT_1402; Fig. 4).

Because of similar electrical resistivity, the boundary between the Quaternary sediments (RU1) and fractured bedrock (RU4) is indistinguishable. Compared to all other ERT lines, the low-resistivity zone has higher

(150–200 Ωm) resistivity at the line ERT_1501 (located south of the Varudi bog, Figs 1, 4) because of (i) the lower degree of fracturing or (ii) an artificial effect due to a thick overlying pile of well conductive Quaternary sediments.

DISCUSSION

Ground-penetrating radar is an efficient tool for describing the shallow subsurface (Davis & Annan 1989; Neal 2004). The GPR studies in Estonia have been carried out mostly in Holocene peat and sand deposits (Plado et al. 2011; Rosentau et al. 2012; Habicht et al. 2017), yet GPR can be effectively used for determining faults, fractures, karst features and overall thickness of the surficial sequence on top of the carbonate bedrock (Dagallier et al. 2000; Jõelet & Plado 2010). Electrical resistivity tomography, which has deeper penetration than GPR, has been frequently applied to detecting the bedrocks below the Quaternary sediments (Giocoli et al. 2008; Chambers et al. 2012), characterizing the faults (Caputo et al. 2003; Bedrosian et al. 2012, Drahor & Berge 2017) and deep valleys (Colella et al. 2004).

Geophysical studies in Viru-Nigula were induced by the ambiguity about the origin and morphology of the Varudi valley. The unusually great thickness of the overburden (30 m) in the Varudi drill core was formerly associated with the buried valley (Suuroja et al. 2006). While the Kunda valley, mapped west of the Varudi bog, is generally well expressed in the modern topography (Fig. 1), the Varudi structure has been entirely filled up and could not be properly located without additional data.

One of the largest Estonian fault networks – the Aseri fault (Fig. 1), with a total length of over 150 km, width 1–4 km and vertical displacement up to 26 m, runs across the study area B3. The uplift of the Aseri's eastern bedrock blocks probably started during the Ediacaran period and continued intermittently later on (Puura & Vaher 1997). Based on drilling data of various oil-shale investigation projects, the main displacement zone of Aseri is only a few hundred metres wide near Viru-Nigula, but fracturing and dislocations may occur in a wider zone. The GPR images of the areas B1 and B3 occasionally show irregular reflections and hyperbolae that may associate with local weathering, karst or faulting. According to the GPR results the top of the bedrock declines abruptly from borehole 1141 towards the SE (Fig. 1). An ERT image (Fig. 3) was accomplished along the same course in order to obtain extra data for the deeper subsurface. As shown in Fig. 3, the GPR and ERT results are in good accordance. While the GPR data show an intermittent (erosional) and descending bedrock top surface, the electrical data indicate a 400 m long bedrock interruption from borehole 1141 to ~850 m SE. Figure 3 also illustrates an efficient approach for geophysical profiling as the relatively rapidly acquired GPR images were useful for locating the time-consuming ERT lines afterwards.

According to the ERT results, the Varudi structure is related to two separate objects of different orientation

(Fig. 5). The northern object, described in three ERT images (Figs 3, 4), is oriented SW–NE. It is about 400 m wide at the northernmost profile (Fig. 3), but becomes narrower in the SW direction and eventually fades out. Such a narrowing of the fracture zone at the ends is typical of faults. Extensive fracturing of the bedrock and thus lower resistance to the Kongla creek's erosion allowed the forming of the incision up to 20 m deep near the Baltic Klint. The contribution of the glacial erosion is rather uncertain.

The southern object, recognized in five ERT images (Fig. 4), is narrower and seems to keep constant width. It is quite straight in the N–S direction. Joining with the northern object presumes sharp turns in a small area between ERT lines 1403 and 1405. At the same time ERT lines 1404 and 1405 exclude its continuation northwards (Fig. 5). In contrast to the northern object, drill core data indicate a thick overburden within the valley structure.

In northern Europe, buried valleys were usually formed by the pre-Quaternary erosion of rivers and were reshaped in several subsequent glaciation periods (Miidel & Raukas 1991; Sandersen & Jørgensen 2003). Miidel et al. (2006) suggest that many of the Estonian valleys were formed in the Late Palaeogene when the ground surface was much higher than today. Such an alluvial erosion hypothesis, however, does not explain the sharp start/end of the Varudi valley. Rattas (2007) analysed the spatial distribution of the bedrock valleys and eskers in northern Estonia and suggested that buried valleys have been important pathways for subglacial meltwater. Moreover, some of the valleys or their segments may be caused by the tunnel valley formation. Occasionally the valleys have an abrupt start and/or end (Rattas 2007) like in the case of the Varudi valley. This can be induced by the glacial outburst flood that occurs when large volumes of subglacially stored water suddenly drain (Benn & Evans 2010). Abruptly terminating deep valleys are more common in southern Estonia, where the Devonian sandstones are easier to erode, than in the carbonaceous rocks of northern Estonia. We speculate that the Varudi valley is located on a fracture zone, which has helped the valley to incise at least 30 m deep into the bedrock.

The outcomes of the current work confirm the connection between faulting and erosion noted by other authors (Hetzel 2013; Ghisetti et al. 2016). Obviously the fractured bedrock described in the ERT images in the Varudi bog and nearby (Figs 3, 4) offered less resistance to the Late Pleistocene glaciers; as the fragmented carbonate beds were outwashed from the bedrock by subglacial waters, glacial and glaciofluvial deposits became their substitutes. Finally in the Holocene, lacustrine sediments and peat accumulated into the remnant depression, thus forming the present bog.

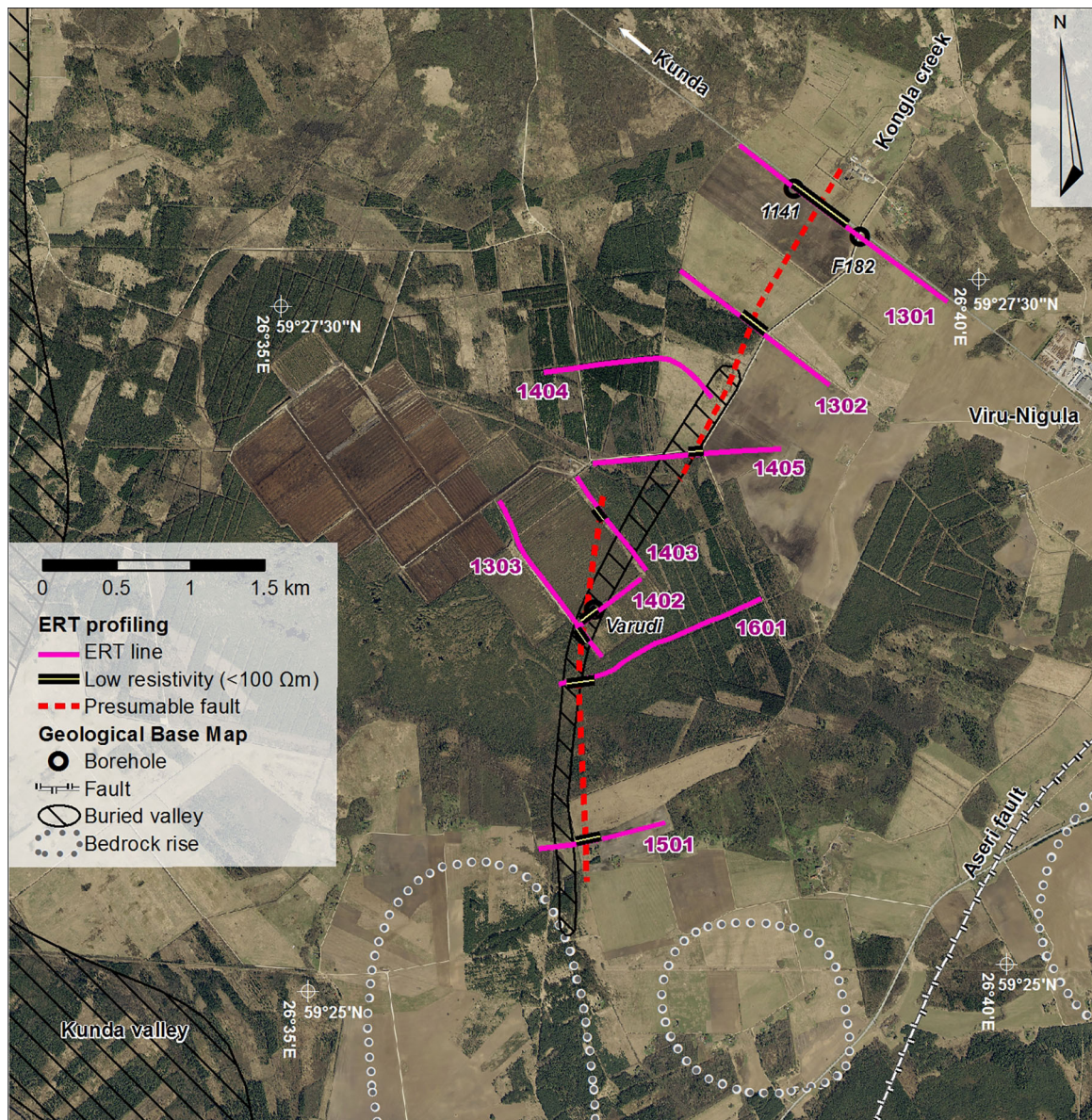


Fig. 5. Location image indicating the ERT lines, low-resistivity (generally $< 100 \Omega\text{m}$) areas and presumable faults according to the electrical measurements. Boreholes, Aseri fault, buried valleys and bedrock rises are from the Geological Base Map (GBM data and orthophoto from the Estonian Land Board).

CONCLUSIONS

Geophysical methods (GPR and ERT) were used for improving the knowledge about the bedrock topography around Viru-Nigula, NE Estonia.

Previously the Varudi valley was defined by an unusually thick pile of Quaternary sediments within the Varudi drill core, however, the genesis of the valley remained unknown (Suuroja et al. 2006). According to the ERT results, the Varudi borehole was drilled into the N–S oriented fracture zone/bedrock incision. The

studies indicate that the Varudi structure consists of two differently oriented incisions provoked by faulting and later filled with Quaternary sediments. During the Late-Pleistocene glaciations they served as flow channels of the fractured, karstified and dissolved sediments, thus clearing the space for the Varudi bog. Subsurface erosion is presently continued by groundwater migration through the fractured areas towards the Kongla creek.

While ERT was practical in deeper situations, GPR offered detailed results in the near-surface environments, enabling (i) specifying the composition of the Quaternary

deposits, (ii) tracing the Ordovician bedrock topography and (iii) recognizing the bedrock dislocations. The authors propose that GPR as a relatively fast method should firstly be applied in similar geological situations, and followed by other surveys (e.g. the ERT) if necessary. Geophysical data acquired during this study allow adjusting the Geological Base Map, likewise assisting in future surveys in the region.

Acknowledgements. The Geological Base Map used as a basis for this work was compiled by the Geological Survey of Estonia and made public by the Estonian Land Board. We thank Kalle Suuroja and Kuldev Ploom from the Estonian Geological Survey for pointing out the need for additional geophysical investigations, for hospitality in the Arbavere field station and competent remarks. We are grateful to the geology students from the University of Tartu who participated in the geophysical fieldwork campaigns in 2012–2016. The two anonymous referees are thanked for constructive reviews of the paper. The study was supported by the Estonian Ministry of Education and Research (grant IUT20-34). The publication costs of this article were covered by the Estonian Academy of Sciences.

REFERENCES

- Bedrosian, P. A., Burton, B. L., Powers, M. H., Minsley, B. J., Phillips, J. D. & Hunter, L. E. 2012. Geophysical investigations of geology and structure at the Martis Creek Dam, Truckee, California. *Journal of Applied Geophysics*, **77**, 7–20.
- Benn, D. I. & Evans, D. J. A. 2010. *Glaciers and Glaciation*. Second edition, Hodder Education, 802 pp.
- Caputo, R., Piscitelli, S., Oliveto, A., Rizzo, E. & Lapenna, V. 2003. The use of electrical resistivity tomographies in active tectonics: examples from the Tyrnavos Basin, Greece. *Journal of Geodynamics*, **36**, 19–35.
- Chambers, J. E., Wilkinson, P. B., Wardrop, D., Hameed, A., Hill, I., Jeffrey, C., Loke, M. H., Meldrum, P. I., Kuras, O., Cave, M. & Gunn, D. A. 2012. Bedrock detection beneath river terrace deposits using three-dimensional electrical resistivity tomography. *Geomorphology*, **177–178**, 17–25.
- Colella, A., Lapenna, V. & Rizzo, E. 2004. High-resolution imaging of the High Agri Valley Basin (Southern Italy) with electrical resistivity tomography. *Tectonophysics*, **386**, 29–40.
- Dagallier, G., Laitinen, A. I., Malartre, F., Van Campenhout, I. P. A. M. & Veeken, P. C. H. 2000. Ground penetrating radar application in a shallow marine Oxfordian limestone sequence located on the eastern flank of the Paris Basin, NE France. *Sedimentary Geology*, **130**, 149–165.
- Davis, J. L. & Annan, A. P. 1989. Ground-penetrating radar for high-resolution mapping of soil and rock stratigraphy. *Geophysical Prospecting*, **37**, 531–551.
- Doolittle, J. A. & Butnor, J. R. 2009. Soils, peatlands, and biomonitoring. In *Ground Penetrating Radar: Theory and Applications* (Jol, H. M., ed.), pp. 179–202. Elsevier.
- Drahor, M. G. & Berge, M. A. 2017. Integrated geophysical investigations in a fault zone located on southwestern part of İzmir city, Western Anatolia, Turkey. *Journal of Applied Geophysics*, **136**, 114–133.
- Ghisetti, F., Sibson, R. H. & Hamling, I. 2016. Deformed Neogene basins, active faulting and topography in Westland: distributed crustal mobility west of the Alpine Fault transpressive plate boundary (South Island, New Zealand). *Tectonophysics*, **693**, 340–362.
- Giocoli, A., Magri, C., Vannoli, P., Piscitelli, S., Rizzo, E., Siniscalchi, A., Burrato, P., Basso, C. & Nocera, S. D. 2008. Electrical resistivity tomography investigations in the Ufita Valley (Southern Italy). *Annals of Geophysics*, **51**, 213–223.
- Habicht, H.-L., Rosentau, A., Jõelet, A., Heinsalu, A., Kriiska, A., Kohv, M., Hang, T. & Aunap, R. 2017. GIS-based multiproxy coastline reconstruction of the eastern Gulf of Riga, Baltic Sea, during the Stone Age. *Boreas*, **46**, 83–99.
- Hetzl, R. 2013. Active faulting, mountain growth, and erosion at the margins of the Tibetan Plateau constrained by in situ-produced cosmogenic nuclides. *Tectonophysics*, **582**, 1–24.
- Jõelet, A. & Kukkonen, I. T. 2002. Physical properties of Vendian to Devonian sedimentary rocks in Estonia. *GFF*, **124**, 65–72.
- Jõelet, A. & Plado, J. 2010. Architecture of the northeastern rim of the Kärđla impact crater, Estonia, based on ground-penetrating radar studies. In *Large Meteorite Impacts and Planetary Evolution IV* (Gibson, R. & Reimold, W. U., eds), pp. 133–140. Geological Society of America, Boulder, Colorado.
- Kalm, V. & Gorlach, A. 2014. Impact of bedrock surface topography on spatial distribution of Quaternary sediments and on the flow pattern of late Weichselian glaciers on the East European Craton (Russian Plain). *Geomorphology*, **207**, 1–9.
- Kirs, J., Puura, V., Soesoo, A., Klein, V., Konsa, M., Koppelmaa, H., Niin, M. & Urtson, K. 2009. The crystalline basement of Estonia: rock complexes of the Palaeoproterozoic Orosirian and Statherian and Mesoproterozoic Calymmian periods, and regional correlations. *Estonian Journal of Earth Sciences*, **58**, 219–228.
- Loke, M. H. & Barker, R. D. 1996. Rapid least-squares inversion of apparent resistivity pseudosections by a quasi-Newton method. *Geophysical Prospecting*, **44**, 131–152.
- Miidel, A. & Raukas, A. 1991. The evolution of the river systems in the East Baltic. In *Temperate Palaeohydrology* (Starkel, I., Gregory, K. J. & Thornes, J. B., eds), pp 365–380. John Wiley & Sons, Chichester.
- Miidel, A., Raukas, A., Tavast, E. & Vaher, R. 2006. Influence of bedrock topography on oil shale mining in North-East Estonia. *Oil Shale*, **23**, 313–327.
- Mustasaar, M., Plado, J. & Jõelet, A. 2012. Determination of electromagnetic wave velocity in horizontally layered sedimentary target: a ground-penetrating radar study from Silurian limestones, Estonia. *Acta Geophysica*, **60**, 357–370.
- Neal, A. 2004. Ground-penetrating radar and its use in sedimentology: principles, problems and progress. *Earth-Science Reviews*, **66**, 261–330.

- Plado, J., Sibul, I., Mustasaar, M. & Jõelet, A. 2011. Ground-penetrating radar study of the Rahivere peat bog, eastern Estonia. *Estonian Journal of Earth Sciences*, **60**, 31–42.
- Plado, J., Preenen, U., Jõelet, A., Pesonen, L. J. & Mertanen, S. 2016. Palaeomagnetism of Middle Ordovician carbonate sequence, Vaivara Sinimäed area, northeast Estonia, Baltica. *Acta Geophysica*, **64**, 1391–1411.
- Puura, V. & Vaher, R. 1997. Tectonics. In *Geology and Mineral Resources of Estonia* (Raukas, A. & Teedumäe, A., eds), pp. 163–180. Estonian Academy Publishers, Tallinn.
- Rattas, M. 2007. Spatial distribution and morphological aspects of eskers and bedrock valleys in North Estonia: implications for the reconstruction of subglacial drainage system under the Late-Weichselian Baltic Ice Stream. *Geological Survey of Finland, Special Paper*, **46**, 63–68.
- Rattas, M. & Kalm, V. 2004. Glaciotectonic deformation patterns in Estonia. *Geological Quarterly*, **48**, 15–22.
- Raukas, A. 1997. Location and topography. In *Geology and Mineral Resources of Estonia* (Raukas, A. & Teedumäe, A., eds), pp. 9–14. Estonian Academy Publishers, Tallinn.
- Raukas, A. & Kajak, K. 1995. Quaternary stratigraphy in Estonia. *Proceedings of the Estonian Academy of Sciences, Geology*, **44**, 149–162.
- Raukas, A. & Kajak, K. 1997. Quaternary cover. In *Geology and Mineral Resources of Estonia* (Raukas, A. & Teedumäe, A., eds), pp. 125–136. Estonian Academy Publishers, Tallinn.
- Rosentau, A., Jõelet, A., Plado, J., Aunap, R., Muru, M. & Eskola, K. O. 2012. Development of the Holocene foredune plain in the Narva-Joesuu area, eastern Gulf of Finland. *Geological Quarterly*, **56**, 89–100.
- Sandersen, P. & Jørgensen, F. 2003. Buried Quaternary valleys in western Denmark – occurrence and inferred implications for groundwater resources and vulnerability. *Journal of Applied Geophysics*, **53**, 229–248.
- Sildvee, H. & Vaher, R. 1995. Geologic structure and seismicity of Estonia. *Proceedings of the Estonian Academy of Sciences, Geology*, **44**, 15–25.
- Suuroja, K.-M., Ploom, K., Mardim, T., All, T., Otsmaa, M., & Veski, A. 2006. *The Explanatory Note to the Geological Maps of Rakvere (6434) Sheet*. Geological Survey of Estonia, Tallinn.
- Tavast, E. 1995. About difficulties in the geophysical investigation of buried valleys in Livonia. In *Geology of Livonia* (Meidla, T., Jõelet, A., Kalm, V. & Kirs, J., eds), pp. 114–118. University of Tartu, Estonian Geological Society, Tartu.
- Tavast, E. 1997. Bedrock topography. In *Geology and Mineral Resources of Estonia* (Raukas, A. & Teedumäe, A., eds), pp. 252–256. Estonian Academy Publishers, Tallinn.
- Vaher, R., Müidel, A. & Raukas, A. 2013. Structure and origin of the Vaivara Sinimäed hill range, Northeast Estonia. *Estonian Journal of Earth Sciences*, **62**, 160–170.

Aluspõhja reljeefi ja rikkevööndite kaardistamine georadari ning eritakistuse tomograafiaga Viru-Nigulas (Kirde-Eestis)

Ivo Sibul, Jüri Plado ja Argo Jõelet

Geofüüsikaliste tööde ajendiks oli varasemalt Eesti Geoloogiakeskuse kaardistajate väljaeraldatud Varudi mattunud org Viru-Nigula lähedal. Valdavalt jääb ümbruskonna puuraukudes pinnakatte paksus mõne meetri piiresse, küündides Varudi rabasse rajatud puuraugus erandlikult 30 meetrini. Oru morfoloogia ja tekkimise kohta täiendava teabe hankimiseks kasutati georadari- ning eritakistuse tomograafia meetodit. Georadariga saadi uusi andmeid pinnakatte paksuse ja koostise ning aluspõhjaliste kivimiplokkide ümberpaigutamise kohta peamiselt kuni 4 m sügavuseni maa-pinnast. Eritakistuse tomograafia (Wenneri ja Wenneri-Schlumbergeri konfiguratsioonid) aitas iseloomustada sügavamaid (kuni 40 m) eritakistuse anomaaliaid. Leiti kaks rikkevööndit, kus tavapäraseid Ordoviitsiumi lubjakivikihid on purustatud ja asendatud pinnakatteliste setetega. Varudi org seondub lõunapoolse vööndiga. Arvatavasti olid mõlemad avastatud rikkevööndid Hilis-Pleistotseenis olulisteks põhjavee ja setete liikumisteedeks, soodustades ühtlasi Varudi raba hilisemat väljakujunemist.